New Dielectric and Ferroelectric Solid Solution of $(1-x)Ba(Mg_{1/3}Nb_{2/3})O_3-xPbTiO_3$ with Morphotropic Phase Boundary

Xifa Long and Zuo-Guang Ye*

Department of Chemistry, Simon Fraser University, 8888 University Drive, Burnaby, BC, V5A 1S6, Canada

Received November 16, 2006. Revised Manuscript Received January 22, 2007

A new solid solution of $(1-x)Ba(Mg_{1/3}Nb_{2/3})O_3-xPbTiO_3$ [$(1-x)$BMN−xPT] has been synthesized in the form of ceramics by solid-state reactions and characterized by means of X-ray diffraction, dielectric spectroscopy, and ferroelectric measurements. A partial solid-state phase diagram of the binary system is established. It exhibits a morphotropic phase boundary region in the composition range between $x = 0.71$ and $x = 0.74$. The dielectric permittivity of BMN has been greatly enhanced by the substitution of PT. The ceramics of 0.4BMN−0.6PT show typical relaxor ferroelectric behavior with the diffuse maximum of high permittivity shifting to higher temperature with increasing frequency. With further increase of the PT content, the permittivity peaks become sharper and frequency-independent, indicating a ferroelectric phase transition, the temperature of which (T_C) increases with x. Thus, the transformation from a simple dielectric, to relaxor, and to ferroelectric phase has been demonstrated in this solid solution system.

1. Introduction

Lead-based perovskite ferroelectric solid solution materials, especially the classes containing $PbTiO_3$ as one of the end components, are of great interest for electromechanical transduction applications due to their superior piezoelectric properties. Single crystals of the relaxor-based $Pb(Mg_{1/3}Nb_{2/3})O_3-PbTiO_3$ (PMN−PT) and $Pb(Zn_{1/3}Nb_{2/3})O_3-PbTiO_3$ (PZN−PT) solid solutions have been investigated extensively in the past few years because of their ultrahigh piezoelectric effects.[1−6] Despite the excellent properties, the PMN−PT and PZN−PT single crystals exhibit a relatively low ferroelectric Curie temperature ($T_C = 140-170$ °C) and an even lower morphotropic phase boundary temperature ($T_{MPB} = 80-110$ °C),[1,6] making the materials to be depoled easily. This inherent drawback decreases the thermal stability of piezoelectric properties and reduces the acoustic power and the operation temperature range of the devices, thus limiting the use of PMN−PT and PZN−PT in many applications. In addition, these materials may cause significant environmental issues because of their high lead content. Therefore, a great deal of effort has been put recently in searching for lead-free or lead-reduced materials with high Curie temperature and good piezoelectric performance.[7−10]

Examination of the composition dependence of the piezoelectric response of the PMN−PT single crystals[11,12] indicates that the highest piezoelectricity occurs in the compositions around the morphotropic phase boundary (MPB), especially close to the boundaries between the rhombohedral and monoclinic phases and the monoclinic and tetragonal phases. This is because the materials of the MPB compositions possess multiple polarization states (dipole orientations) which can be switched more susceptibly to an electric field drive, making the materials more electrically active, thereby enhancing the piezoelectric response. In addition, the energy coupling effect between two MPB phases with close energy states makes it possible to yield an ultrahigh coupling coefficient. In piezoelectric materials, high coupling coefficients means high piezoelectricity. Therefore, to find new materials which exhibit high dielectric, piezoelectric, and ferroelectric performance and a high T_C, it is necessary to search for novel solid solution systems with formation of morphotropic phase boundary. Eitel et al.[13] found that, for a large number of $PbTiO_3$ (PT)-based solid solutions, the T_C of the MPB compositions decreases linearly as the tolerance factor of the other end members increases (see Figure 7), suggesting that a solid solution whose other end member has a relatively low tolerance factor tends to exhibit a higher MPB Curie temperature. This empirical relation provides guidance in search for new high T_C solid solution systems.

* Corresponding author. Phone: (604)291-3351. Fax: (604)291-3765. E-mail: zye@sfu.ca.

(1) Park, S.-E.; Shrout, T. R. *J. Appl. Phys.* **1997**, *82*, 1804.
(2) Dong, M.; Ye, Z.-G. *J. Cryst. Growth.* **2000**, *209*, 81.
(3) Luo, H.; Xu, G.; Wang, P.; Yin, Z. *Ferroelectrics* **1999**, *231*, 97.
(4) Kumar, F. J.; Lim, L. C.; Chilong, C.; Tan, M. J. *J. Cryst. Growth* **2000**, *216*, 311.
(5) Rajan, K. K.; Ng, Y. S.; Zhang, J.; Lim, L. C. *Appl. Phys. Lett.* **2004**, *85*, 4136.
(6) Kuwata, J.; Uchino, K.; Nomura, S. *Ferroelectrics* **1981**, *37*, 579.
(7) Makiuchi, Y.; Aoyagi, R.; Hiruma, Y.; Nagata, H.; Takenaka, T. *Jpn. J. Appl. Phys.* **2005**, *44*, 4350.
(8) Cheng, J.; Meng, Z.; Cross, L. E. *J. Appl. Phys.* **2004**, *96*, 6611.
(9) Takenaka, T.; Nagata, H. *J. Eur. Ceram. Soc.* **2005**, *25*, 2693.
(10) Guo, Y.; Kakimoto, K.; Ohsato, H. *Solid State Commun.* **2004**, *129*, 279.
(11) Feng, Z.; Zhao, X.; Luo, H. *J. Phys.: Condens. Matter* **2004**, *16*, 6771.
(12) Bokov, A.; Ye, Z.-G. Unpublished.
(13) Eitel, R. E.; Randall, C. A.; Shrout, T. R.; Rehrig, P. W.; Hackenberger, W.; Park, S.-E. *Jpn. J. Appl. Phys.* **2001**, *40*, 5999.

10.1021/cm062733+ CCC: $37.00
Published on Web 02/15/2007

$Ba(Mg_{1/3}Nb_{2/3})O_3$ (BMN), a lead-free member of the complex perovskite $A(B'B'')O_3$ family,[14,15] has been given much attention as a candidate for microwave dielectric materials due to its high dielectric constant and very low dielectric loss tangent at room temperature.[16−18] We believe that BMN can present some features of the relaxors (PMN or PZN) so as to form a solid solution with ferroelectric $PbTiO_3$ (PT), in which a morphotropic phase boundary is expected to exist, and thereby the dielectric and ferroelectric properties of the materials may be enhanced. In addition, the lead content will be reduced compared with the PMN−PT and PZN−PT solid solutions. This paper reports the synthesis, phase analysis, and dielectric and ferroelectric characterizations of the ceramics of the new $(1-x)Ba(Mg_{1/3}Nb_{2/3})O_3-xPbTiO_3$ solid solution, and the establishment of the solid-state phase diagram of the system, which reveals the existence of a morphotropic phase boundary region.

2. Experimental Section

The ceramics of the $(1-x)Ba(Mg_{1/3}Nb_{2/3})O_3-xPbTiO_3$ solid solution were prepared by solid solution reactions with the compositions of $x = 0$, 0.3, 0.4, 0.5, 0.6, 0.65, 0.7, 0.71, 0.72, 0.73, 0.74, 0.75, 0.8, 0.9, and 1. A two-step synthetic process was used. First, pure BMN and PT were synthesized separately at 1300 and 1000 °C, respectively, for 4 h, from the starting materials of $BaCO_3$, MgO, Nb_2O_5, PbO, and TiO_2 (99.9%). Second, the solid solutions of the desired compositions were prepared by mixing and thoroughly grinding the appropriate amounts of BMN and PT and calcining at the temperatures of 1000−1100 °C for 6 h. The calcined powders were then reground and pressed into pellets and sintered at 1000−1250 °C for 4 h (ramp rate = 5 °C/min) in a sealed Al_2O_3 crucible to form the ceramics.

A Rigaku R-axis diffractometer was employed to determine the formation of the $(1-x)$BMN−xPT solid solution. A Radiant RT-66A standard ferroelectric test system was used to measure the polarization−electrical field (P−E) hysteresis loop. The dielectric constant and dielectric loss were measured at various frequencies using a Solartron 1290 impedance analyzer in conjunction with a 1296 dielectric interface, with an ac voltage of 0.5 V_{rms}. The measurements were carried out as a function of temperature upon heating from −100 to 300 °C by means of a Delta Chamber (Model 9023).

3. Results and Discussion

3.1. X-ray Diffraction. Figure 1 shows the X-ray diffraction pattern of the $(1-x)$BMN−xPT ceramics with selected compositions of $x = 0-1$. The following can be seen: (1) all samples with different compositions crystallize in a pure perovskite phase, free of impurities; (2) the compositions with $x = 0.70$ and smaller exhibit a rhombohedral (pseudo-cubic) symmetry, reflecting the disordered structure of BMN; (3) the compositions with $x = 0.75$ and higher show the splitting of the pseudo-cubic (100), (110), (200), and other peaks, and this splitting becomes more significant for the compositions with $x = 0.80$, 0.90, and 1.0, indicating a tetragonal symmetry for the solid solution with a high PT content; (4) for $x = 0.71-0.75$, the (100) and (200) peaks first become broadened and asymmetrical and then split at $x = 0.75$, suggesting that the symmetry of the phase gradually changes from rhombohedral to tetragonal upon increasing PT content from $x = 0.70$ to $x = 0.75$. Therefore, a morphotropic phase boundary (MPB) region is indeed present within this composition range (see section 3.3).

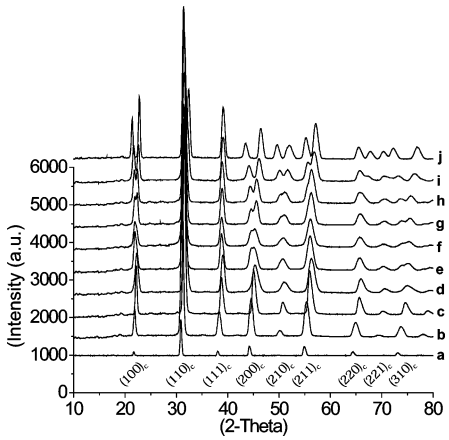

Figure 1. X-ray diffraction patterns of the $(1-x)$BMN−xPT ceramics (a: $x = 0$, b: $x = 0.3$, c: $x = 0.6$, d: $x = 0.7$ e: $x = 0.71$, f: $x = 0.74$, g: $x = 0.75$, h: $x = 0.8$, i: $x = 0.9$, j: $x = 1$).

Figure 2 shows, as an example, the experimental XRD data (open circles) of the pseudo-cubic (200) reflection for the compositions of $x = 0.70$, 0.73, and 0.75. The peak profile is deconvoluted with the tetragonal and/or rhombohedral phase components. It can be seen that, for $x = 0.70$, the (200) reflection is composed of a single peak, corresponding to the rhombohedral phase. For $x = 0.73$, the (200) reflection is composed of three peaks, with the dominant peaks 1 and 2 corresponding to the tetragonal phase and the broad and weak peak 3 arising from the residual rhombohedral phase. For $x = 0.75$, the tetragonal symmetry can be clearly identified by the two distinct peaks, while the rhombohedral peak has completely disappeared. This phase analysis result confirms that the tetragonal and rhombohedral phases coexist within the MPB region ($0.70 < x < 0.75$) and the tetragonal phase component gradually increases at the expense of the rhombohedral phase as the PT content increases.

Table 1 gives the densities of the $(1-x)$BMN−xPT ceramics with compositions of $x = 0.3$, 0.4, 0.5, 0.6, 0.7, and 0.75 (the experimental densities were measured using density bottle method and the theoretical densities were calculated using lattice parameters from X-ray diffraction data). It can be seen that the relative density of all the samples consistently reached 92−94%, making the comparative studies of the dielectric properties of the solid solution system meaningful.

3.2. Dielectric Properties and Phase Transitions. The circular surfaces of the $(1-x)$BMN−xPT ceramic samples were polished and sputtered with gold layers on both sides as electrodes for electrical measurements. The temperature and frequency dependencies of the dielectric permittivity were measured on ceramics. The complex dielectric permit-

(14) Lufaso, M. W. *Chem. Mater.* **2004**, *16*, 2148.
(15) Dias, J. J.; Vimala, T. M.; Murthy, V. R. K. *Jpn. J. Appl. Phys.* **2002**, *41*, 3010.
(16) Gupta, S. M.; Furman, E.; Colla, E.; Xu, Z.; Viehland, D. J. *J. Appl. Phys.* **2000**, *88*, 2836.
(17) Akbas, M. A.; Davies, P. K. *J. Am. Ceram. Soc.* **1998**, *81*, 670.
(18) Liu, H. X.; Tian, Z. Q.; Wang, H.; Yu, H. T.; Ouyang, S. X. *J. Mater. Sci.* **2004**, *39*, 4319.

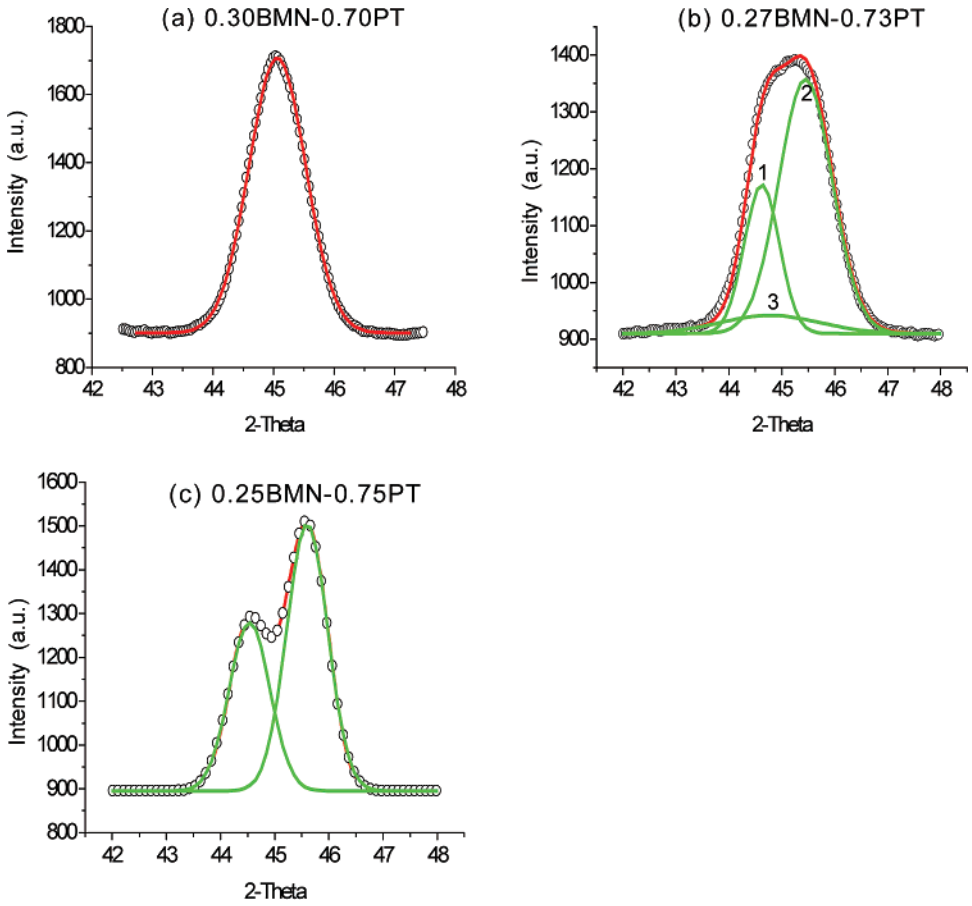

Figure 2. Pseudo-cubic (200) reflection (open circles) of (1−*x*)BMN−*x*PT with compositions of $x = 0.7$ (a), 0.73 (b), and 0.75 (c), at room temperature. The peak profile is deconvoluted with the rhombohedral (a) or tetragonal (c) phase, or a mixture of the two phases (b).

Table 1. Density of the (1−*x*)BMN−*x*PT Ceramics of Different Compositions

x	theoretical density (g/cm^3)	measured density (g/cm^3)	relative density
0.3	6.68	6.23	0.93
0.4	6.85	6.27	0.92
0.5	7.04	6.51	0.922
0.6	7.25	6.74	0.93
0.7	7.5	6.98	0.93
0.75	7.49	7.02	0.94

tivity of the unpoled (as-sintered) ceramics with the compositions of $x = 0.2-0.9$ were measured as a function of temperature at the frequencies of $f = 1$, 10, and 100 kHz. Figure 3shows the variations of the real permittivity (dielectric constant) and loss tangent for $x = 0.4$, 0.6, 0.7, and 0.74. It can be seen that the spectral features depend closely on the composition. For $x \leq 0.5$ (Figure 3a), the dielectric constant remains low (<1000) and no anomaly appears in the temperature range from −120 to 300 °C. For $x = 0.6$ (Figure 3b), interestingly, the dielectric constant shows a broad maximum with frequency dispersion, the temperature of which (T_{max}) shifts to higher temperatures with increasing frequency, indicating a typical relaxor behavior.[19−21] Moreover, the value of the dielectric constant is increased dramatically and reaches about 4000 at T_{max} which is close to room temperature. For $x = 0.7$ and higher (Figures 3c and 3d), the relaxor behavior transforms into normal ferroelectric character with a frequency-independent sharp dielectric peak and almost nondispersive permittivity values, indicating the phase transition from the tetragonal or rhombohedral ferroelectric phase to the cubic paraelectric phase upon heating. As the PT content increases, the ferroelectric T_C moves to higher temperatures toward the T_C of pure PT.

The variations of the dielectric constant and loss tangent for the BMN−PT ceramics with compositions $x = 0.3$, 0.4, 0.5, 0.6, 0.65, 0.70, 0.71, 0.72, 0.73, 0.74, 0.75, and 1 at room temperature are given in Figure 4. It can be seen that the dielectric loss decreases slightly with the PT content increasing up to $x = 0.3$. It then increases with further increase of x, more significantly at $x > 0.7$, resulting from the effect of PT. On the other hand, the dielectric constant increases to a maximum value of about 4000 at $x = 0.60$, which arises from the relaxor behavior induced by the PT substitution, with the diffuse maximal dielectric constant appearing near room temperature.

Figure 5 presents the real permittivity as a function of temperature at the frequency of 100 kHz for the selected compositions of $x = 70$, 72, 73, 74, and 75 mol % PbTiO$_3$. A broad peak of the real permittivity appears at the ferroelectric Curie temperature, T_C (or T_{max}) = 235, 245, 255, and 265 °C, respectively, indicating that T_C (or T_{max}) increases almost linearly as a function of the PT content for the MPB compositions. These temperatures also define the upper limit of the MPB region (see below). Interestingly,

(19) Cross, L. E. *Ferroelectrics* **1987**, *76*, 241.
(20) Ye, Z.-G. *Key Eng. Mater.* **1998**, *155*−156, 81.
(21) Bokov, A. A.; Ye, Z.-G. *J. Mater. Sci.* **2006**, *41*, 31.

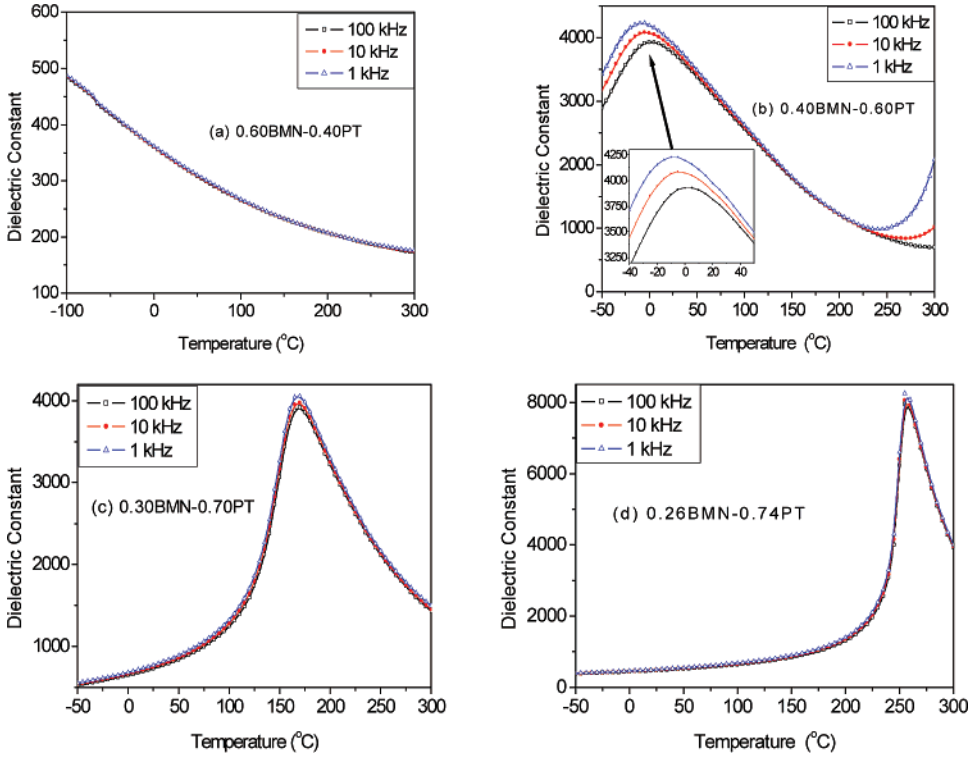

Figure 3. Dielectric constant of the (1−*x*)BMN−*x*PT ceramics as a function of temperature for the compositions $x = 0.40$ (a), 0.60 (b), 0.70 (c), and 0.74 (d), measured at the frequencies of $f = 1$, 10, and 100 kHz.

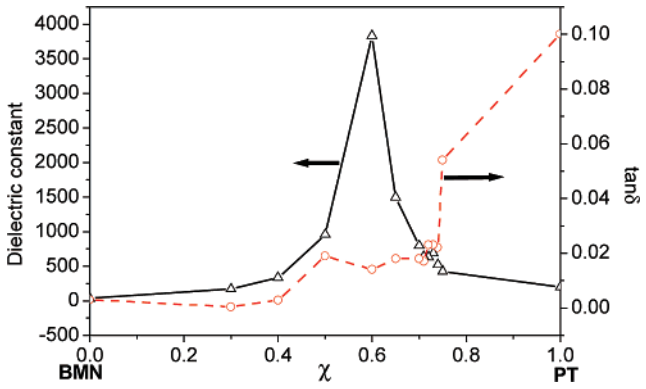

Figure 4. Dielectric constant and loss tangent for the (1−*x*)BMN−*x*PT ceramics at room temperature as a function of the composition.

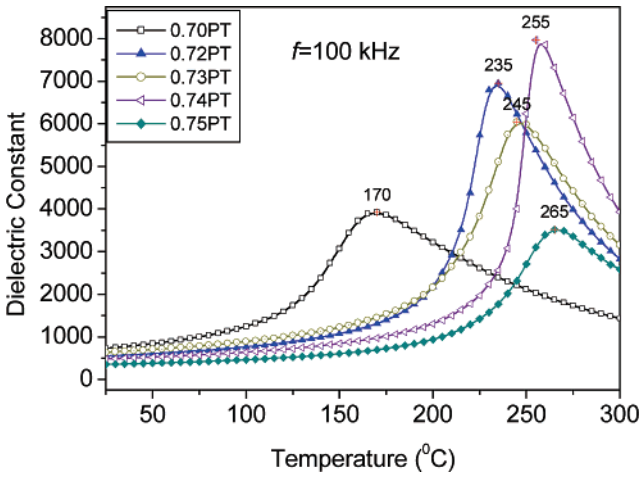

Figure 5. Real permittivity as a function of temperature for the (1−*x*)-BMN−*x*PT solid solution with $x = 0.70$, 0.72, 0.73, 0.74, and 0.75, measured at the frequency $f = 100$ kHz.

the compounds of the MPB compositions display a $T_C >$ 200 °C, which is higher than that of the PMN−PT and PZN−PT solid solutions.

3.3. Morphotropic Phase Diagram of the (1-*x*)BMN−*x*PT Solid Solution System. Based on the above XRD and dielectric results, the solid-state temperature (T) vs composition (x) phase diagram of the (1−*x*)BMN−*x*PT binary system in the composition range of $0.6 \leq x \leq 1.0$ has been established, as shown in Figure 6. It delimits the stability regions for the cubic paraelectric phase, the rhombohedral relaxor phase, and the tetragonal ferroelectric phase. The most important feature of this phase diagram is that a morphotropic phase boundary region exists in the composition range of $0.71 \leq x \leq 0.74$, where the rhombohedral phase and the tetragonal phase coexist. Therefore, as the amount of PT increases, the (1−*x*)BMN−*x*PT solid solution undergoes (at room temperature) the sequence of structural transformation from the rhombohedral phase ($x < 0.71$), to a mixture of the rhombohedral and tetragonal phases ($0.71 \leq x \leq 0.74$) and then to the tetragonal phase ($x > 0.74$). Note that MPB was originally defined as a compositional dividing line between two adjacent phases of different symmetry in the temperature vs composition phase diagram of such solid solution systems as $PbZr_{1-x}Ti_xO_3$[22] and PMN−PT.[23] Our results show that the morphotropic phase behavior with coexistence of two phases occurs within a composition range in the BMN−PT system, which is similar to the revised morphotropic phase diagrams for the PMN−PT[24] and PZN−

(22) Jaffe, B.; Cook, W. R., Jr.; Jaffe, H. *Piezoelectric Ceramics*; Academic Press: London, 1971.
(23) Choi, S. W.; Shrout, T. R.; Jang, S. J.; Bhalla, A. S. *Ferroelectrics* **1989**, *100*, 29.
(24) Noheda, B.; Cox, D. E.; Shirane, G.; Gao, J.; Ye, Z.-G. *Phys. Rev. B* **2002**, *66*, 054104.

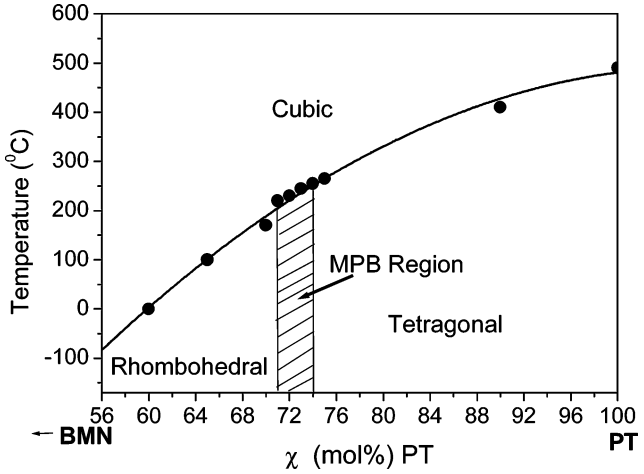

Figure 6. Partial phase diagram for the (1−*x*)BMN−*x*PT solid solution system, showing the presence of a MPB region for 0.71 < *x* < 0.74.

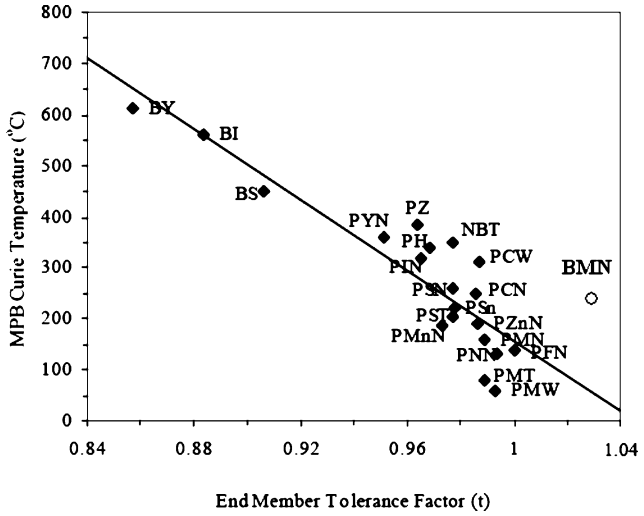

Figure 7. Relationship scheme of the T_C of PT-based MPBs versus the tolerance factor of (the other) end member [after ref 13]. Open circle shows the point for the BMN−PT system from this work.

PT[25] systems (for historical reasons, we keep the term "morphotropic phase boundary" and extend it to "MPB region").

The tolerance factor of BMN was calculated to be 1.03 using Shannon's ionic radii. According to Eitel's relationship,[13] the MPB Curie temperature of the present BMN−PT system should be lower than 50 °C. However, interestingly, the actual T_C is found to be higher than 200 °C, as reported in this work. We believe that such a discrepancy arises most likely because the Eitel's relationship deals with the solid solutions of (A-site) Bi^{3+}- and Pb^{2+}-based end members (with PT), whereas the BMN−PT system involves a Ba^{2+}-based end member. The differences in the ionicity, ionic radius, and bonding nature between the Ba^{2+} ion and the Pb^{2+} and Bi^{3+} ions of peculiar features (with lone pair electrons) suggest that the BMN−PT system does not necessarily follow the linear relationship depicted for the Bi^{3+}- and Pb^{2+}-based systems. Instead, a new relationship needs to be established for the Ba^{2+}-based solution solutions with PT. And the result of the present work provides a starting point for such a relationship.

(25) La-Orauttapong, D.; Toulouse, J.; Ye, Z.-G.; Chen, W.; Erwin R.; Robertson, J. L. *Phys. Rev. B* **2003**, *67*, 134110.

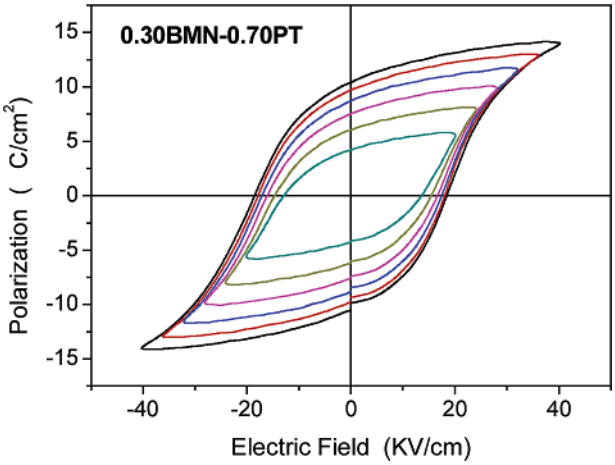

Figure 8. Dielectric hysteresis loops displayed on a 0.30/0.70 BMN/PT solid solution ceramic at various bipolar electric fields applied.

To illustrate this interesting observation, the relation between the MPB T_C and the end member tolerance factor of the BMN−PT system is indicated in Figure 7 together with the Bi^{3+}- and Pb^{2+}-based systems after ref 13. It can be seen that the BMN point is situated above the linear trend. This suggests that by reduction of the tolerance factor, the Ba^{2+}-based solutions with PT might exhibit higher T_C than the Bi^{3+}- and Pb^{2+}-based systems.

3.4. Ferroelectricity. The measurements of the polarization as a function of alternating electric field reveal well-developed hysteresis loops, indicating that the BMN−PT solid solution samples with compositions near the MPB are ferroelectric at room temperature. Figure 8 shows the hysteresis loops displayed for the 0.30/0.70 BMN/PT ceramics at different bipolar electric fields applied. It can be seen that the hysteresis loops become more saturated with increasing field strength. The remnant polarization reaches $P_r \approx 10\ \mu C/cm^2$ under a drive of $E \approx \pm 40$ kV/cm, with a coercive field of $E_C \approx 18$ kV/cm.

4. Conclusions

A new solid solution of (1−*x*)BMN−*x*PT has been synthesized by solid-state reaction and characterized by dielectric and ferroelectric measurements. The partial solid-state *T*− *x* phase diagram of the binary system has been established based on the structural and dielectric characterizations. A morphotropic phase boundary region is found to exist within the composition range of $0.71 \leq x \leq 0.74$. Upon increasing PT content, the solid solution displays a spectrum of properties from simple dielectric, to relaxor, and to ferroelectric. The compounds of the MPB compositions exhibit a $T_C > 200$ °C, which is higher than that of the PMN−PT and PZN−PT solid solutions, making the BMN−PT system promising high Curie temperature and lead-reduced materials for potential piezo- and ferroelectric applications.

Acknowledgment. This work was supported by the Natural Science and Engineering Research Council of Canada (NSERC).

CM062733+